The Plant Cell, Vol. 22: 91–107, January 2010, www.plantcell.org

The *ABORTED MICROSPORES* Regulatory Network Is Required for Postmeiotic Male Reproductive Development in *Arabidopsis thaliana* [W] [OA]

Jie Xu,[a] Caiyun Yang,[b] Zheng Yuan,[a,b] Dasheng Zhang,[a] Martha Y. Gondwe,[b] Zhiwen Ding,[a] Wanqi Liang,[a] Dabing Zhang,[a,c,1,2] and Zoe A. Wilson[b,2]

[a] School of Life Science and Biotechnology, Shanghai Jiao Tong University, Shanghai 200240, China
[b] School of Biosciences, University of Nottingham, Sutton Bonington Campus, Loughborough, Leicestershire, LE12 5RD, United Kingdom
[c] Bio-X Research Center, Key Laboratory of Genetics and Development and Neuropsychiatric Diseases, Ministry of Education, Shanghai Jiao Tong University, Shanghai 200240, China

The *Arabidopsis thaliana ABORTED MICROSPORES* (*AMS*) gene encodes a basic helix-loop-helix (bHLH) transcription factor that is required for tapetal cell development and postmeiotic microspore formation. However, the regulatory role of *AMS* in anther and pollen development has not been fully defined. Here, we show by microarray analysis that the expression of 549 anther-expressed genes was altered in *ams* buds and that these genes are associated with tapetal function and pollen wall formation. We demonstrate that AMS has the ability to bind in vitro to DNA containing a 6-bp consensus motif, CANNTG. Moreover, 13 genes involved in transportation of lipids, oligopeptides, and ions, fatty acid synthesis and metabolism, flavonol accumulation, substrate oxidation, methyl-modification, and pectin dynamics were identified as direct targets of AMS by chromatin immunoprecipitation. The functional importance of the AMS regulatory pathway was further demonstrated by analysis of an insertional mutant of one of these downstream AMS targets, an ABC transporter, White-Brown Complex homolog, which fails to undergo pollen development and is male sterile. Yeast two-hybrid screens and pull-down assays revealed that AMS has the ability to interact with two bHLH proteins (AtbHLH089 and AtbHLH091) and the ATA20 protein. These results provide insight into the regulatory role of the AMS network during anther development.

INTRODUCTION

Anther and pollen development is a complex biological process that includes a series of crucial events that require cooperative interactions between gametophytic and sporophytic genes (Goldberg et al., 1993, 1995; McCormick, 2004; Scott et al., 2004; Ma, 2005; Wilson and Zhang, 2009). The mature anther consists of four lobes, each containing meiotic cells at the center surrounded by four somatic cell layers (i.e., the outermost epidermis, the endothecium, the middle layer, and the innermost tapetum) (Goldberg et al., 1993).

The tapetum is in direct contact with the developing gametophytes (Pacini et al., 1985; Shivanna et al., 1997) and plays a vital secretory role in the development of microspores to pollen grains, such as providing enzymes for the release of microspores from tetrads, nutrients for pollen development, and pollen wall components (Goldberg et al., 1993). During the late stages of pollen development, the tapetum undergoes cellular degradation via programmed cell death (PCD) (Papini et al., 1999; Wu and Cheun, 2000; Li et al., 2006a). Tapetal aberrations are frequently observed in male sterile mutants (Kaul, 1988), with premature or delayed degradation of the tapetum resulting in male sterility.

Several transcription factors have been demonstrated to regulate postmeiotic tapetal development. The rice (*Oryza sativa*) *UNDEVELOPED TAPETUM1* gene and its putative *Arabidopsis thaliana* ortholog *DYSFUNCTIONAL TAPETUM1* (*DYT1*), encoding basic helix-loop-helix (bHLH) transcription factors, were shown to be crucial for tapetal differentiation and the formation of microspores (Jung et al., 2005; Zhang et al., 2006). It has been proposed that DYT1 may directly regulate the *ABORTED MICROSPORE* (*AMS*) and *MALE STERILITY1* (*MS1*) genes (Zhang et al., 2006) that play critical roles in regulating downstream events of tapetal and microspore development. Chromatin immunoprecipitation (ChIP)-PCR and binding studies have recently confirmed the direct regulation of MS1 by DYT1 (H. Ma, personal communication). *MS1* encodes a plant homeodomain transcription factor that is briefly expressed from the late tetraspore to free microspore stage (Yang et al., 2007). Numerous expression changes have been detected in the *ms1* mutant, particularly in genes associated with the deposition of pollen wall materials (Alves-Ferreira et al., 2007; Ito et al., 2007; Yang et al., 2007). Tapetal development was also shown to be altered in this mutant, with a lack of normal PCD and change to autophagic

[1] Address correspondence to zhangdb@sjtu.edu.cn.
[2] The research groups of these authors contributed equally to this work. The authors responsible for distribution of materials integral to the findings presented in this article in accordance with the policy described in the Instructions for Authors (www.plantcell.org) are: Zoe A. Wilson (zoe.wilson@nottingham.ac.uk) and Dabing Zhang (zhangdb@sjtu.edu.cn).
[W] Online version contains Web-only data.
[OA] Open Access articles can be viewed online without a subscription.
www.plantcell.org/cgi/doi/10.1105/tpc.109.071803

tapetal degeneration occurring (Vizcay-Barrena and Wilson, 2006).

The *AMS* gene encodes a postmeiotic, tapetally expressed bHLH protein (Sorensen et al., 2003), which also has a putative ortholog in rice, *Tapetum Degeneration Retardation* (*TDR*) (Li et al., 2006a; Zhang et al., 2008). The *ams* mutant displays an expanded tapetal layer and aborted microspores (Sorensen et al., 2003), while the *tdr* mutation has been shown to delay tapetal degeneration and PCD, as well as result in microspore collapse (Li et al., 2006a).

To clarify the functional role of AMS in anther and microspore development, we performed microarray analysis on the *ams* mutant and showed that AMS regulates the expression of a number of genes involved in various biological activities, particularly those associated with metabolism and deposition of the pollen wall. Moreover, 13 genes involved in tapetal development and pollen wall formation have been shown by ChIP-PCR analysis to be direct regulatory targets of AMS. The functional importance of this pathway has further been demonstrated by analysis of an insertional mutant of one of these downstream AMS targets, an ATP Binding Cassette (ABC) transporter, White-Brown Complex homolog protein 27 (WBC27). Mutants of *WBC27* result in a failure of pollen development and male sterility, while other aspects of development remain unaffected. Furthermore, using yeast two-hybrid screens and pull-down assays, AMS has been shown to interact with two bHLH proteins (AtbHLH089 and AtbHLH091) and the tapetum-specific ATA20 protein. This work provides insight into the regulatory role of AMS in plant male reproductive development.

RESULTS

Transcriptome Analyses of Wild-Type and *ams* Anthers

To identify the downstream targets and establish the role of AMS during *Arabidopsis* pollen development, we employed microarray analysis using RNA from wild-type and *ams* buds. Four developmental stages, based on microscopy analysis, were analyzed, namely, prior to and including meiosis, pollen mitosis I, bicellular, and pollen mitosis II. The expression data were converted to two color log ratios. Therefore, a negative value represents downregulation compared with expression of the wild type. Significance analysis of microarray (SAM) (Tusher et al., 2001) was used to identify differentially expressed genes, a false discovery cutoff of <5% was used for the initial selection of candidate genes, and a secondary filtering of >log2 fold difference was then applied.

Compared with the wild-type buds, 759 genes (SAM analysis, false discovery rate <5%; see Supplemental Data Set 1 online) exhibited expression changes during the four anther developmental stages in the *ams* mutant. Among these genes, 134 were downregulated more than twofold prior to and during the meiosis stage, 189 during the pollen mitosis I stage, 189 during the bicellular pollen stage, and 155 during the pollen mitosis II stage. However, of these 759 genes, only 549 (see Supplemental Data Set 1 online) were identified as being expressed in the *Arabidopsis* anther based upon staged microarray analysis of wild-type *Arabidopsis* anthers (NASC Affymetrix arrays, http://affymetrix.arabidopsis.info/narrays/experimentbrowse.pl). In addition, of the 549 genes, 366 were also expressed in the pollen (Honys and Twell, 2004), while 183 were expressed in the anther but were not detectable within the pollen transcriptome set.

Expression data obtained from the array hybridization were also verified by quantitative RT-PCR (qRT-PCR) using independently generated samples and genes selected because they had high fold change and/or functional relevance (i.e., *ABC* transporter, *LTP12*, At*bHLH089*; see Supplemental Figure 1 online). The correlations between the fold changes observed from the RT-quantitative PCR (qPCR) closely mirrored those obtained in the microarray analysis, confirming the reliability of the microarray data.

In the wild type, *AMS* gene expression occurs for a prolonged period, commencing during early meiosis and continuing through to immediately prior to flower opening (pollen mitosis II stage) (see Supplemental Figure 1A online), which agrees with a previous *AMS-Promoter:β-glucuronidase* expression analysis (Sorensen et al., 2003). In the *ams* mutant, a general reduction in gene expression was observed throughout the period of normal *AMS* expression. *K* mean clustering of the 549 genes identified groups of genes that were coordinately expressed at the various developmental stages (Figure 1). These included 37 genes that were slightly downregulated at the mitosis I stage but showed an increased downregulation at the bicellular and mitosis II stage (Cluster 2), 32 genes downregulated at all four stages (Cluster 4), 80 genes downregulated only at the mitosis I stage (Cluster 5), 75 genes downregulated only at the bicellular stage (Cluster 6), 53 genes downregulated at meiosis, mitosis I, and bicellular stages but no change at the mitosis II stage (Cluster 7), and 84 genes downregulated only at the mitosis II stage (Cluster 10).

The expression of early genes associated with anther development, including *EXTRA SPOROGENOUS CELLS/EXCESS MICROSPOROCYTES1* (*EXS/EMS1*) (Canales et al., 2002; Zhao et al., 2002), *MS5* (Glover, et al., 1998), *MYB33* and *MYB65* (Millar and Gubler, 2005), and *SPOROCYTELESS/NOZZLE* (*SPL/NZZ*) (Schiefthaler et al., 1999; Yang et al., 1999), was not significantly changed in the *ams* mutant (Table 1). Several genes that exhibit expression changes in the *ams* buds are known to be associated with later pollen development, including *MS2* (Aarts et al., 1997), *ARABIDOPSIS THALIANA ANTHER20* (*ATA20*), *ATA7* (Rubinelli et al., 1998), *ATA1* (Lebel-Hardenack et al., 1997), *ARABIDOPSIS THALIANA SUGAR TRANSPORTER* (*ATSTP2*) (Truernit et al., 1999), *POLY(A) BINDING PROTEIN5* (*PAB5*) (Belostotsky and Meagher, 1993), *CYTOCHROME P450 CYP704B1* (Dobritsa et al., 2009), *CYP703A2* (Morant et al., 2007), and *Acyl-CoA Synthetase 5* (*ACOS5*) (Souza et al., 2009) (Table 1; see Supplemental Data Set 1 online), suggesting that AMS may modulate anther development by either directly or indirectly regulating these genes.

Expression Changes of Genes Involved in Pollen Wall Formation in *ams* Anthers

The 549 genes showing altered expression in the *ams* mutant were functionally grouped (The Arabidopsis Information

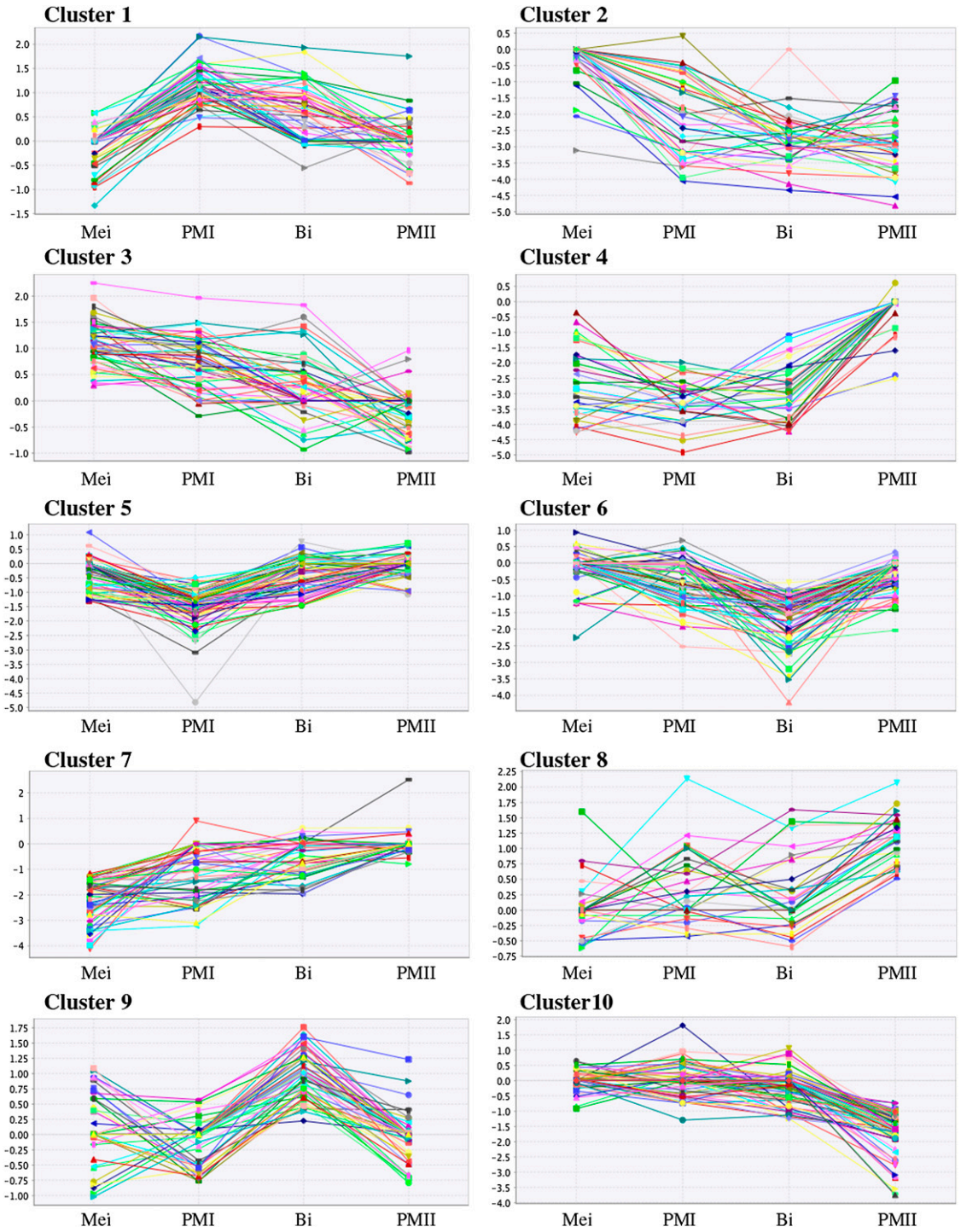

Figure 1. The 549 Genes That Showed Altered Expression in the *ams* Mutant Were Clustered into 10 Groups by *K*-Mean Clustering.

Columns from left to right in each cluster are expression profiles of the meiosis and earlier stages (Mei), the pollen mitosis I stage (PMI), the bicellular stage (Bi), and the pollen mitosis II stage (PMII), respectively. The *y*-axes show relative expression compared with wild-type expression. Cluster 1: Genes were slightly upregulated at the meiosis stage, greatly in the mitosis I and bicellular stages, and less at the mitosis II stage in the *ams* mutant. Cluster 2: Downregulated genes, slightly at the mitosis I stage but greatly at bicellular and mitosis II stages. Cluster 3: Genes upregulated at meiosis, mitosis I, and bicellular stages but slightly downregulated at the mitosis II stage. Cluster 4: Genes downregulated at all four stages. Cluster 5: Genes downregulated only at the mitosis I stage. Cluster 6: Genes downregulated only at the bicellular stage. Cluster 7: Genes downregulated at meiosis, mitosis I, and bicellular stages but no change at the mitosis II stage. Cluster 8: Genes upregulated only at the mitosis II stage. Cluster 9: Genes upregulated only at the bicellular stage. Cluster 10: Genes downregulated only at the mitosis II stage.

Table 1. Expression in the *ams* Mutant of Genes Previously Reported to Be Altered by *EMS1/EXS* and *MS1* Expression and to Be Involved in Anther Development

Gene Name	Locus	Description	Fold Change in *ems1*[a]	Change of Expression in *dyt1*[a]	Fold Change in *ms1* Young Buds[a]	Fold Change in *ams* Young Buds			
						Mei	PM I	Bi	PM II
SPL	At4g27330	SPL/NZZ	−3	0	1	1	1	1	1
EMS1	At5g07280	EMS1/EXS	−7	0	1	1	1	1	1
MS5	At4g20900	Male sterility MS5; pollenless3	−3	0	1	1	1	1	1
SDS	At1g14750	SOLO DANCER, a putative cyclin	−3	0	1	1	1	1	1
MYB33	At5g06100	MYB family transcription factor (MYB33)	1	0	1	1	1	1	1
MYB65	At3g11440	MYB family transcription factor (MYB65)	−2	0	1	1	1	1	1
bHLH089	At1g06170	Basic helix-loop-helix (bHLH) family protein	−33	0	1	−3	−2	1	1
MS5-like gene	At5g44330	MS5 family protein	−60	Down	1	1	1	1	1
	At5g07230	Protease inhibitor/seed storage/lipid transfer protein, tapetum-specific protein A9	−63	Down	1	−14	−2	1	1
MS2	At3g11980	MS2	−56	Down	1	−18	2	1	1
ATA1	At3g42960	Alcohol dehydrogenase (ATA1)	−70	Down	2	−8	1	1	1
	At3g13220	ABC transporter	−55	Down	2	−6	1	−4	1
LTP12	At3g51590	Lipid transfer protein	−11	Down	−52	−13	−8	−19	1
ATSTP2	At1g07340	Hexose transporter	−3	Down	−3	−1	−2	1	1
PAB5	At1g71770	Polyadenylate binding protein	−8	Down	−2	1	1	−4	1
CYP704B1	At1g69500	Cytochrome P450	−97	–	3	−12	1	1	1
CYP703A2	At1g01280	Cytochrome P450	−48	–	14	−10	1	1	1
ACOS5	At1g62940	Acyl-CoA Synthetase 5	−54	–	1	−7	1	1	1
A6	At4g14080	Glycosylhydrolase family 17 protein / anther-specific protein (A6)	−90	–	3	−12	1	1	1
UBQ1	At3g52590	UBIQUITIN EXTENSION PROTEIN 1 (UBQ1)	1	1	1	1	1	1	1

[a]Data are taken from Yang et al. (2007), Wijeratne et al. (2007), and Zhang et al. (2006); –, not analyzed. UBQ1 was used as a control.

Resource; http://www.Arabidopsis.org/) into four categories of (1) information storage and processing, (2) cellular processes and signaling, (3) metabolism, and (4) genes of unknown functions (Table 2; see Supplemental Figure 2 online). A high proportion of these were associated with metabolism, transcription, cell wall/membrane/envelope biogenesis, posttranslational modification, and signal transduction (Table 2).

The *AMS* gene is specifically expressed in the tapetum, with high expression during pollen mitosis I and the bicellular microspore stages (Sorensen et al., 2003). The tapetum is metabolically active and plays a major role in pollen development by contributing to microspore release, nutrition, pollen wall synthesis, and pollen coat deposition. Mutations of regulators of tapetal development cause expression changes of a large number of genes related to lipid, carbohydrate, and amino acid metabolism. For instance, the *tdr* mutant anther displayed a total of 236 significantly changed genes compared with the wild type, of which 95 genes were related to metabolism (Zhang et al., 2008). Consistently, we observed that the expression of 89 genes predicted to be involved in lipid metabolism, carbohydrate and amino acid transport, and metabolism was downregulated (42.4% of the total 210 downregulated genes; Table 2; see Supplemental Table 1 online) at the mitosis I stage in the *ams* mutant.

Enzymatic conversion is a core event for lipid metabolism. In *ams*, the expression of 30 genes encoding enzymes putatively involved in lipid synthesis was altered (29 downregulated and one upregulated). In planta, de novo biosynthesis of fatty acids occurs in plastids using two enzyme systems (i.e., heteromeric acetyl-CoA carboxylase and fatty acid synthase), which result in acyl-ACP moieties that are 16 or 18 carbons long (O'Hara et al., 2001). The activity of acyl-CoA synthetase has been shown to vary coincidentally with levels of fatty acids during lipid accumulation in rice seed (Ichihara et al., 2003). In the *ams* anther, we observed a decrease in the expression of At1g21540, At2g36190, At5g07680, and At5g60020 (acyl-CoA synthetase), and At2g07560 (acyl-CoA reductase), which are all thought to be involved in fatty acid synthesis and metabolism.

The conversion of fatty alcohols from fatty acids is required for wax and ether lipid synthesis, which is essential for the establishment of the elaborate pollen wall in flowering plants. *MS2*, encoding a putative fatty acyl reductase, is expressed in the tapetum during pollen development in *Arabidopsis*. MS2 is thought to convert fatty acids into fatty alcohols during the production of sporopollenin, and the *ms2* mutant exhibits abnormal exine development (Aarts et al., 1997). In the *ams* mutant, we observed a dramatic reduction in *MS2* expression at the meiosis stage (see Supplemental Data Set 1 online).

Table 2. Functional Classification by EuKaryotic Orthologous Group Analysis of Genes with Altered Expression in the *ams* Mutant as Identified by SAM Analysis (<5% False Discovery Rate) and Showing a >Log2-Fold Change in Expression (for detailed function of gene, see Supplemental Data Set 1)

Function	Down	Mei	PMI	Bi	PMII	UP	Mei	PMI	Bi	PMII	Total
Information storage and processing											
Translation, ribosomal structure, and biogenesis	17	3	6	5	3	7	4	1	0	2	24
RNA processing and modification	11	2	4	5	0	1	0	1	0	0	12
Transcription	29	2	8	10	9	4	2	1	0	1	33
Chromatin structure and dynamics	3	1	1	1	0	1	0	1	0	0	4
Cellular processes and signaling											
Cell cycle control, cell division, chromosome partitioning	1	0	0	1	0	0	0	0	0	0	1
Defense mechanisms	31	7	8	3	13	14	1	3	10	0	45
Signal transduction mechanisms	41	8	17	6	10	32	7	4	19	2	73
Cell wall/membrane/envelope biogenesis	35	6	14	8	7	13	1	0	5	7	48
Cytoskeleton	10	2	4	2	2	4	0	1	2	1	14
Extracellular structures	1	0	0	0	1	3	1	1	1	0	4
Intracellular trafficking, secretion, and vesicular transport	1	0	0	0	1	2	0	1	1	0	3
Posttranslational modification, protein turnover, chaperones	41	18	7	9	7	21	5	8	5	3	62
Metabolism											
Energy production and conversion	11	0	4	7	0	2	1	1	0	0	13
Carbohydrate transport and metabolism	58	11	14	19	14	30	8	11	6	5	88
Amino acid transport and metabolism	38	8	12	15	3	5	1	3	1	0	43
Nucleotide transport and metabolism	8	2	2	3	1	0	0	0	0	0	8
Coenzyme transport and metabolism	7	2	2	2	1	1	0	0	0	1	8
Lipid transport and metabolism	82	14	22	25	21	14	7	4	2	1	96
Inorganic ion transport and metabolism	25	10	8	3	4	11	4	4	3	0	36
Secondary metabolites biosynthesis, transport and catabolism	97	28	28	29	12	20	6	7	5	2	117
Poorly characterized											
General function prediction only	119	34	37	27	21	113	18	29	33	33	232
Function unknown	32	7	12	8	5	73	14	16	28	15	105

Transport of lipidic molecules from the tapetum to microspore surface is considered to be essential for pollen wall formation. The expression of two genes putatively related to lipid transport (At3g51590, a lipid transfer protein type 1, LTP type 1, and At1g66850, LTP type 2) was significantly reduced in *ams*. Three pollen oleosin genes (At5g07510, At5g07520, and At5g07550) associated with pollen wall development were also downregulated in *ams*. Oleosins represent >90% of the detectable *Arabidopsis* and *Brassica* pollen proteome (Mayfield et al., 2001) and have been shown to be critical in the formation of the pollen wall and the subsequent germination of pollen grains (Mayfield and Preuss, 2000; Hsieh and Huang, 2007; Jiang et al., 2007).

AMS Alters the Expression of Genes Required for Tapetal Differentiation and Degradation

Tapetal cell differentiation and subsequent disintegration coincides with the anther postmeiotic developmental program. Semithin microscopy analysis was performed on stage 5 to 11 anthers to confirm that the *ams* Salk knockout had a similar phenotype as the previously reported *ams* mutant (Sorensen et al., 2003) and to provide a more detailed analysis of the *ams* phenotype. During stage 5, the anthers of the wild type and *ams* mutant appeared similar, although the callose wall surrounding the *ams* tetrads was slightly more pronounced (see Supplemental Figures 3A and 3E online). However, at stage 7, the *ams* anther displayed more vacuolated and irregular tapetal cells compared with the wild type (see Supplemental Figures 3B and 3F online). At stage 9, the wild-type tapetum appeared condensed, while the *ams* tapetal layer and other anther wall layers, such as the epidermis and endothecium, looked more vacuolated, and the microspores degenerated, with no visible pollen exine (see Supplemental Figures 3C and 3G online). From stage 11, mature, round pollen grains were observed in the locules of wild-type anthers, whereas the *ams* anther wall was vacuolated and greatly expanded, with no developed microspores (see Supplemental Figures 3D and 3H online). Consistently, our transmission electron micrograph (TEM) analysis indicated that the wild-type anther displayed degenerated tapetal cells (see Supplemental Figure 4A online) and pollen grains that formed pollen exine (see Supplemental Figure 4B online) at stage 11. However, the *ams* mutant anther appeared to be delayed in tapetal cell degradation (see Supplemental Figure 4C online), and the locule contained degenerated pollen grains with no detectable pollen exine (see Supplemental Figure 4D online).

Structurally, the most severe defect of *ams* was an abnormally large and delayed degenerated tapetum (see Supplemental Figures 3 and 4 online), suggesting that the *ams* mutant underwent aberrant tapetal cell differentiation and PCD. Likewise, in the *tdr* mutant, we found that tapetal PCD was retarded (Li et al., 2006a). The predicted effectors that carry out cell death–associated processes in animals include proteases, nucleases, and reactive oxygen species (Wu and Cheun, 2000). In the microarray data, we observed several senescence-associated

genes that exhibit altered expression in *ams*, with one senescence-associated gene (At5g66170) showing increased expression levels in the mutant. Cys proteases are known to participate in various physiological and developmental processes in plants (Li et al., 2006a). Previously, we showed that TDR can directly bind the promoter region of rice *CP1*, which encodes a Cys protease, suggesting that Cys proteases are likely effectors of tapetal PCD in plants. In this study, the expression of three genes encoding Cys proteases (At4g16190, At1g06260, and At4g36880) was shown to be reduced in *ams*.

A group of tapetal-specific transcription factors have been reported to play key roles in tapetal and pollen development (Ma, 2005). In the *ams* mutant, 15 putative transcription factors were shown to exhibit altered expression (i.e., bHLH transcription factor, hematopoietically expressed homeobox transcription factor, and MYB family transcription factors) (see Supplemental Table 2 online), suggesting that AMS may, at least in part, regulate tapetal development via other transcription factors.

Genes associated with carbohydrate transport and metabolism showed altered expression in the *ams* mutant; for example, the putative hexose transporters (At3g05960, At1g07340, and At1g50310), sugar transporter proteins (SUC1/At1g71880, At5g18840, and At3g05400), sugar carrier protein (At1g77210), and invertase-like protein (At4g34860). In plants, sucrose is the major transport form of photoassimilated carbon, which serves as a source of carbon skeletons and energy for plant organs (sink organs) (Lemoine, 2000). Some other gene products thought to be involved in the tricarboxylic acid cycle pathway (e.g., β-galactosidase, β-glucosidase, galactokinase, glucosyltransferase, glycosylhydrolase, and galactosyltransferases) were also altered in *ams* (see Supplemental Table 1 online).

Additionally, downregulation of genes related to amino acid transport and metabolism, such as the putative amino acid transporters At5g04770, At2g38905, and At1g71770, was observed in the *ams* mutant. Other gene products thought to be involved in the amino acid metabolism pathway, such as At1g06250 (Tyr amino transferase), At3g23840 (Asn synthase), At1g23600 (Gln synthetase), At3g42850 (Ala-glyoxylate amino transferase AGT2), At1g23520 (Glu/Leu/Phe/Val dehydrogenases), and At3g57810 (isovaleryl-CoA dehydrogenase), were also downregulated. In addition, the expression of several APG (a Pro-rich protein)-like genes was altered in *ams* (see Supplemental Data Set 1 online). The tapetum-specific *APG* gene in *Silene latifolia* was previously shown to be associated with the development of fertile pollen (Ageez et al., 2005).

AMS Has the Ability to Bind E-Box CANNTG

AMS is a putative bHLH transcription factor. The basic region is located at the N terminus of the bHLH domain and functions as a DNA binding motif. It consists of ~15 amino acids, which typically include six basic residues (Atchley et al., 1999). The bHLH region contains two amphipathic helices with a linking loop of variable lengths; the amphipathic helices of two bHLH proteins can interact, allowing the formation of homodimers or heterodimers (Nesi et al., 2000). Some bHLH proteins have been shown to bind to sequences containing a consensus core element called the E box (CANNTG), with the G box (CACGTG) being the most common form. In addition, the nucleotides flanking the core element may also have a role in binding specificity (Atchley et al., 1999; Martinez-Garcia et al., 2000; Massari and Murre, 2000; Robinson et al., 2000).

To determine whether AMS specifically associates with a DNA motif, we employed and modified an efficient and easy approach for identifying the DNA binding sequence specificity of novel plant transcription factors as described by Xue (2005). A C-terminal glutathione *S*-transferase (GST)-AMS fusion protein was prepared from the full-length *AMS* open reading frame (ORF). The GST fusion protein (Figure 2A; molecular mass of 88 kD) was purified using glutathione sepharose (see Supplemental Figure 5A online) and incubated with a pool of double-stranded degenerate oligonucleotides according to Xue (2005). The protein-DNA complexes were washed, the eluted DNA molecules were amplified by PCR (see Supplemental Figure 5B online), and the resulting products were incubated with GST-AMS fusion protein for the next cycle of selection. After five rounds of selection and amplification, the PCR products were cloned and sequenced (see Supplemental Figure 5B online). Of the 38 cloned sequences, 27 were unique and 21 contained the 6-bp consensus AMS binding DNA motif sequence CANNTG (Figure 2C; see Supplemental Figure 5C online).

AMS Directly Binds the Promoter Regions of 13 Genes Involved in Anther Development

To further reveal the regulatory role of AMS during *Arabidopsis* pollen development, the 1000-bp upstream region of the 549

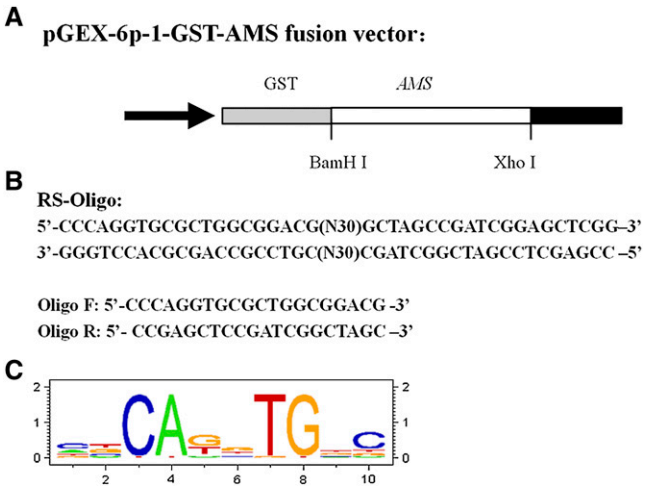

Figure 2. Assay of AMS Binding Sites.

(A) Schematic representation of the AMS-GST fusion construct. The *Xho*I and *Bam*HI sites in pGEX-4T-GST were used as cloning sites for insertion of the *AMS* gene.

(B) Random sequence oligonucleotides (RS-Oligo) used for target binding site selection. Oligo F is a sequence-specific sense primer, and Oligo R is a sequence-specific antisense primer, which were used for PCR amplification of AMS-selected oligonucleotides.

(C) Canonical AMS binding motif analyzed by WebLogo (Web-based sequence logo generating application; Weblogo.berkeley.edu).

genes found to have altered expression in the *ams* microarray analysis was analyzed for the presence of E-box binding motifs (CANNTG) (see Supplemental Data Set 2 online). The results showed that the promoters of 150 genes (27.32%) contained more than five E-box binding motifs within the 1-kb upstream region of each gene, while the promoter regions of 124 genes (22.59%) and 107 genes (19.49%) contained three or four motifs, respectively. The remaining 165 genes (30.06%) had less than two motifs in the promoter regions. The high ratio of occurrence of the CANNTG motif in these genes is not so surprising since statistically the frequency of occurrence of the motif CANNTG is ~1 in 128 nucleotides. To confirm the binding ability of AMS with these candidate genes, we employed ChIP-PCR analysis on 73 selected putative targets that showed downregulation in the microarray analysis and the presence of the predicted E-box binding motifs in their promoter regions (see Supplemental Data Set 2 online).

Polyclonal antibodies were prepared using a recombinant AMS fragment with low similarity to other proteins. Protein gel blot analysis confirmed that the AMS antibody reacts exclusively with the AMS protein, giving the expected wild-type-sized band (see Supplemental Figure 6, lane 2, online) and no detectable signal in the *ams* mutant (see Supplemental Figure 6, lane 3, online). Quantitative ChIP-PCR (qChIP-PCR) showed specific enrichment when the affinity-purified AMS antibodies were used compared with when no AMS antibodies were used for the selected upstream regions of 13 genes (Table 3) out of the 73 putative target genes tested (Figure 3). This, combined with the downregulation of these genes in the *ams* mutant (Table 3), suggests that AMS directly regulates the expression of these 13 genes. According to *K*-mean cluster classification, eight of these belong to Cluster 4, which contains genes that were downregulated during all four stages of pollen development (Figure 1).

Among these genes, four appear to be involved in lipid transport and metabolism: At3g51590 (a lipid transfer protein type 1), At1g66850 (a lipid transfer protein type 2), At5g49070 (a fatty acid elongase/3-ketoacyl-CoA synthase), and At1g75920 (a predicted lipase). This further confirms the crucial role of AMS in regulating lipid synthesis and transport during pollen wall development. *Arabidopsis CYP703A2* belongs to a cytochrome P450 family conserved in land plants, which is required for pollen exine formation (Morant et al., 2007). In the *ams* anther, the expression of *CYP703A2* was decreased during the early stages of pollen development. Furthermore, the expression of 10 additional P450 members belonging to CYP71/76/81/83/86/98/703/704/705/707/709 was altered in *ams* (see Supplemental Table 3 online). Of these, two (At1g13140 and At3g28740) appear to be directly regulated by AMS, as indicated by the enrichment for the promoter regions of these sequences by qChIP-PCR (Figure 3). These results demonstrate the crucial role of AMS in regulating biosynthetic pathways for pollen development.

Flavonol accumulation is essential for pollen development; in petunia (*Petunia hybrida*), a lack of chalcone synthase (CHS) results in an absence of flavonols and male sterility (Pollak et al., 1993). In the *ams* mutant, two putative *CHS* genes (At4g34850 and At4g00040) and five genes encoding flavonol reductase/cinnamoyl-CoA reductases (At1g23060, At1g75220, At2g29340, At2g42990, and At5g40350) were found to be downregulated. Furthermore, qChIP-PCR indicates that AMS can bind to the promoter region of the putative *CHS* gene, At4g00040 (Figure 3).

AMS was also shown to directly regulate *At1g75790*, a member of the multicopperoxidase family, a putative H+/oligopeptide symporter (At1g59740), and synaptic vesicle transporter-like gene (At1g73220) (Figure 3), suggesting a potential role in pollen wall formation and male reproductive development.

The ABC Transporter WBC27, Which Is Regulated by AMS, Is Essential for Pollen Wall Development

To further confirm the qChIP-PCR data that AMS directly regulates the ABC transporter WBC27 (Figure 3), we performed an electrophoretic mobility shift assay (EMSA) with AMS and the promoter region (−213 to −37) of the ABC transporter *WBC27*. A supershifted band was observed in the *WBC27* promoter region sample when incubated with the recombinant AMS protein (see Supplemental Figure 7, lanes 2 and 3, online), whereas no supershifted signal was observed in the control sample containing the pGEX-4T-1 control plasmid (see Supplemental Figure 7, lane 1, online). Moreover, we observed a decreased signal when a 25- and 100-fold molar excess of unlabeled *WBC27* probe (see

Table 3. List of Representative AMS Binding Targets as Shown by ChIP-qPCR That Were Differentially Expressed in the *ams* Microarray Analysis.

Genes Positively Regulated by AMS		Mei	PMI	Bi	PMII	Cluster Group
At1g59740	H^+/oligopeptides symporter	−1.19	−2.18	−2.27	−0.86	4
At3g51590	Lipid transfer protein type 1	−3.68	−2.98	−4.24	0.00	4
At1g66850	Lipid transfer protein type 2	−4.08	−4.92	−4.10	−1.09	4
At1g75920	Predicted lipase	−3.12	−3.58	−4.06	0.00	4
At5g49070	Fatty acid elongase/3-ketoacyl-CoA synthase	−1.01	−0.66	0.00	0.00	5
At1g75790	Multicopperoxidase	−3.09	−3.36	−2.79	0.00	4
At1g67990	*O*-methyltransferase	−4.22	−3.90	−3.86	0.00	4
At4g00040	Chalcone synthase	−0.45	−1.30	0.00	0.00	5
At3g28740	Cytochrome P450 CYP2 subfamily	0.00	1.14	1.34	0.18	1
At1g13140	Cytochrome P450 CYP4/CYP19/CYP26 subfamilies	−1.77	−2.78	−1.57	−0.07	4
At5g17050	UDP-glucuronosyl and UDP-glucosyl transferase	−1.50	−1.08	−1.01	0.00	7
At3g13220	Transporter, ABC superfamily (Breast cancer resistance protein)	−2.57	0.00	−1.95	0.00	7
At1g73220	Synaptic vesicle transporter SVOP and related transporters (major facilitator superfamily)	−1.74	−3.09	−2.14	−1.60	4

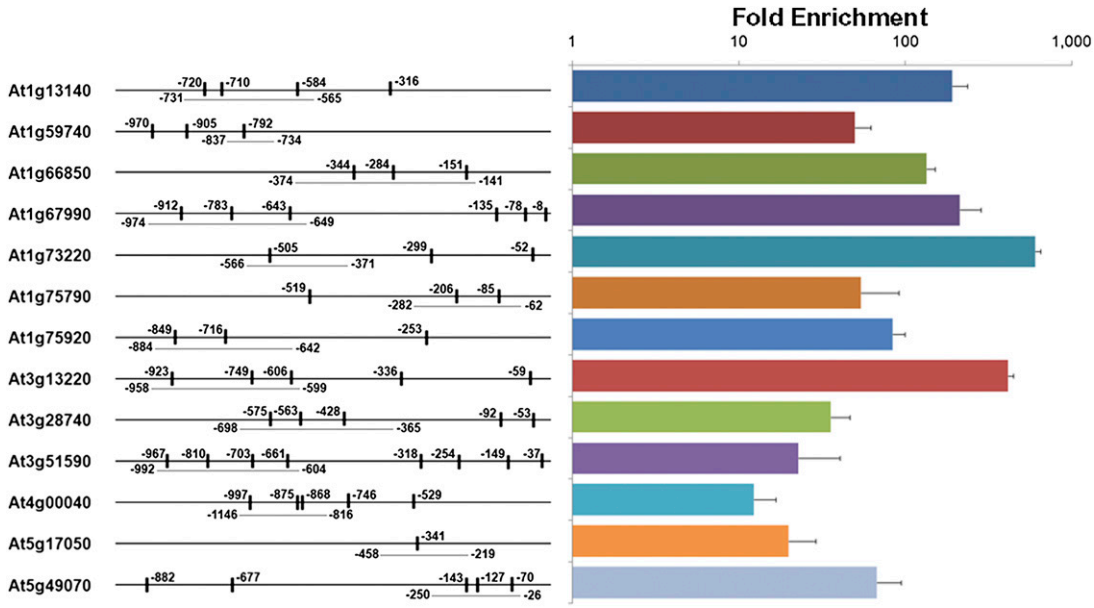

Figure 3. qChIP-PCR Analysis of the Enrichment of AMS Regulatory Targets and the Predicted E-Boxes in Their Promoter Regions.

Fold enrichment calculations from qPCR assays in three independent ChIP experiments. The predicted E-boxes are indicated as vertical black lines in the promoter regions of the AMS targets, and the PCR amplicons used for ChIP-qPCR containing the E-boxes are underlined. Fold enrichment data were analyzed to calculate the fold change between the ChIP (anti-AMS immune serum) and no-antibody control, and all of the targets tested were present at higher amounts in the sample with anti-AMS immune serum than in the no-AMS antibody preimmune precipitation.

Supplemental Figure 7, lanes 3 and 4, online) were added as competitor to the EMSA reaction. This result further confirms that AMS directly regulates the expression of the ABC transporter WBC27 in planta. Analysis of Affymetrix array data indicates that WBC27 is preferentially expressed in the developing inflorescence (https://www.genevestigator.com), and qRT-PCR indicates that, like *AMS*, *WBC27* is expressed during early anther development (see Supplemental Figure 1A online). Consistent with the expression pattern of *AMS* in tapetal cells (Sorensen et al. 2003), *Promoter:β-glucuronidase* and in situ analyses of the WBC27 ABC transporter indicate that *WBC27* is specifically expressed in the tapetum (D. Ye, personal communication), providing further evidence that the expression of ABC transporter *WBC27* is regulated by AMS during anther development.

ABC transporters belong to the ABC superfamily, which use the hydrolysis of ATP to transport a variety of substances across biological membranes. The *Arabidopsis* genome encodes 120 ABC-transporter proteins, which are classified into 13 subfamilies. WBC27 is part of the WBC/ABCG (white/brown complex) subfamily, which is the largest subfamily in *Arabidopsis* (Sanchez-Fernandez et al., 2001; Jasinski et al., 2003; Garcia et al., 2004; Rea, 2007). WBC family transporters have previously been linked to the excretion of lipids (Lu et al., 2007; Luo et al., 2007; Panikashvili et al., 2007), and it is therefore likely that WBC27 plays a role in lipid transport.

To investigate the function of the ABC transporter WBC27, the SALK insertional mutant (SALK_062317), which carries a T-DNA insert in the fifth exon of At3g13220, was genotyped, and homozygous knockouts were analyzed by qRT-PCR for expression of the AT3g13220 transcripts and for phenotypic changes (Figure 4). The knockout plants developed normally until flowering, at which point self-fertilization did not occur and the siliques remained small and lacked seeds (Figures 4B and 4D). Free microspores were visible in the immature anthers of the *wbc27* mutant (Figure 4H); however, they lacked the defined shape of the wild-type microspores and appeared to have a more diffuse tapetal composition (Figure 4G). The microspores subsequently degenerated so that the mature anthers lacked functional pollen (Figure 4J), with the mature anthers appearing shrivelled and small and failing to dehisce (Figures 4F and 4J). However, female fertility was unaffected, and the plants could be rescued using wild-type pollen. No expression of the *WBC27* transcript was observed in the homozygous insertional lines (Figure 4K). We observed that the *WBC27* knockout results in a male sterile phenotype due to microspore degradation (Figure 4). It is therefore interesting to learn of a recent independent report that TEM and scanning electron microscopy analysis of the WBC27/At3g13220 insertional mutant indicated abnormal pollen wall development during microspore/pollen formation and that this male sterile defect was rescued by the genomic DNA of *WBC27* (D. Ye, personal communication), supporting the hypothesis that WBC27 may be involved in the transport of lipidic precursors associated with sporopollenin biosynthesis.

Comparison of the Regulatory Role of AMS with That of SPL, EMS1, and MS1 during Anther Development

SPL/NZZ is one of the earliest expressed genes known to be essential for anther cell division and differentiation (Schiefthaler et al., 1999; Yang et al., 1999) and, when mutated, results in

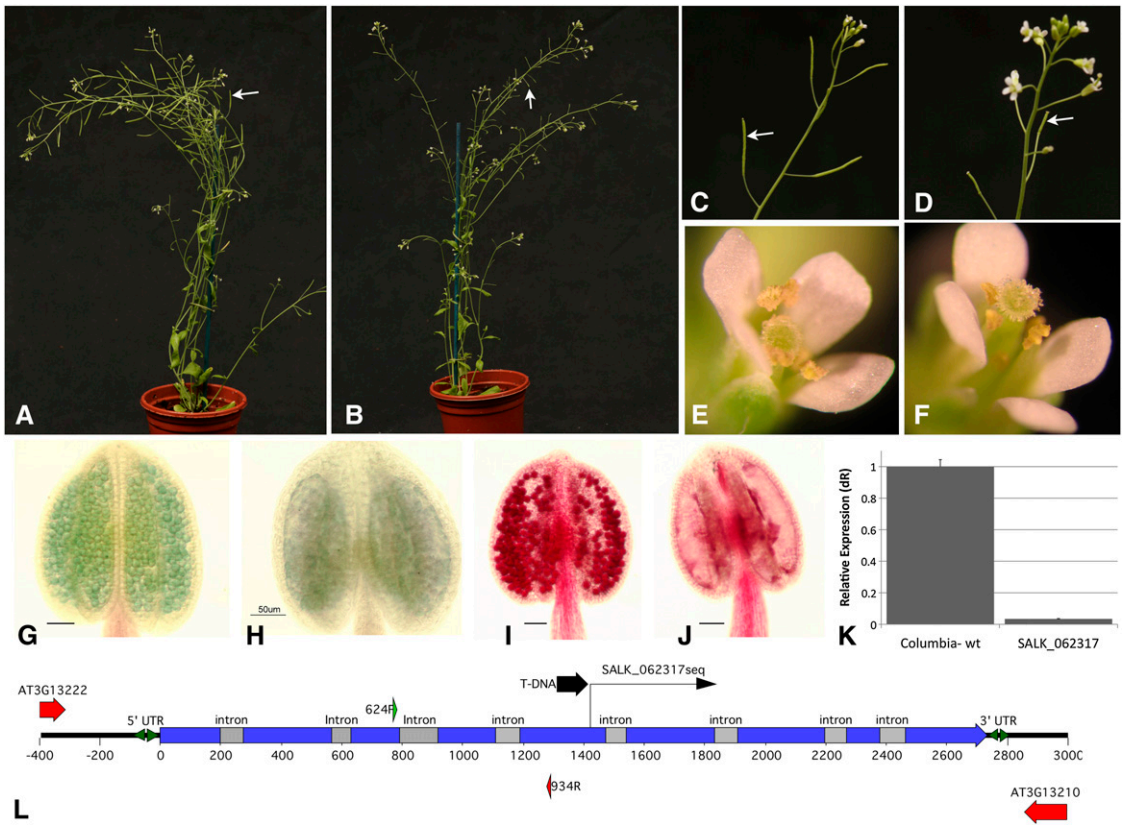

Figure 4. Analysis of ABC Transporter *WBC27* Knockout.

(A) and **(C)** Columbia wild-type plant with normal silique development (arrows).
(B) and **(D)** The *wbc*27/SALK_062317 homozygous mutant, showing reduced silique elongation (arrows).
(E) Wild-type flower containing dehisced anthers.
(F) Mature *wbc*27/SALK_062317 mutant flower containing shrivelled anthers that fail to dehisce.
(G) Immature wild-type anther containing newly released microspores.
(H) Immature *wbc27*/SALK_062317 mutant anther containing abnormal immature microspores, which lack the defined shape of the wild-type microspores. Excessive amounts of material are visible in the locule, suggesting abnormal tapetal development.
(I) Alexander-stained mature wild-type anther showing viable pollen grains.
(J) Alexander-stained mature*wbc*27/SALK_062317 mutant anther lacking viable pollen.
(K) qRT-PCR of *WBC27* expression in the Columbia wild-type and *wbc27*/SALK_062317 mutant inflorescences, indicating that only trace levels of expression were observed in the *wbc27* mutant. Expression was normalized to *ACTIN7* and presented relative to wild-type expression levels and was based upon a minimum of two biological replicates; error bars represent SD.
(L) SALK-062317 T-DNA insertion position in At3g13220. Blue arrow represents coding sequence of At3g13220, gray boxes represent introns, black arrow shows sequenced T-DNA flanking region, black arrowhead shows approximate T-DNA insertion point, and red and green arrows show primers used for qRT-PCR.
Bars in **(G)** to **(J)** = 50 μm.

abnormal male and female sporocyte differentiation. *EXS/EMS1* is another gene required for early tapetal initiation (Canales et al., 2002; Zhao et al., 2002). The *exs/ems1* mutants have increased numbers of archesporial cells and no tapetal and middle cell layers. Transcriptomic analysis indicated that the expression of 1954 and 525 genes was changed in the *spl* and *ems1* mutants, respectively (Wijeratne et al., 2007). Given that *SPL* acts earlier than *EMS1*, the difference in the number of changed genes between these mutants suggests the relative regulatory position of these genes of during pollen development; *SPL* acts very early in the pollen development (stage 2), followed by *EMS1* (stages 2 to 4), and subsequently *AMS* and *MS1* (stages 6 to 8) (Yang et al., 2007) regulate late anther development. Of the 549 genes that were differentially expressed in the *ams* mutant, the expression of 198 genes was also changed in the *spl* and *ems1* mutants (see Supplemental Data Set 3 online). The remaining 351 genes are likely to be involved in anther development independently of *SPL* and *EMS1*; for example, chalcone synthase (At1g24600), a cytochrome P450 CYP2 subfamily member (At1g27770), and soluble epoxide hydrolase (At3g51000) only showed downregulation in the *ams* mutant.

Microarray comparisons were also made between genes previously shown to have altered expression in the *ms1* mutant (Alves-Ferreira et al., 2007; Yang et al., 2007) and those with altered expression in *ams*. We observed that 152 of 361 genes downregulated in the *ams* mutant were also downregulated in the *ms1* mutant (see Supplemental Data Set 4, Supplemental Figure 8, and Supplemental Table 4 online). These genes are predicted to act in lipid transport and metabolism (15 genes, 9.6% of total downregulated genes; see Supplemental Table 1 online), amino acid transport and metabolism (nine genes, 5.9%), secondary metabolite biosynthesis (12 genes, 7.9%), and carbohydrate transport and metabolism (five genes, 3.3%). Despite *MS1* and *AMS* both functioning during the late stages of pollen development, the observed differences in downstream gene expression suggest distinct regulatory roles for these two genes during anther development.

AMS Interacts with AtbHLH089/091 and ATA20

Recently, a SET domain protein, ASH1-Related3 (ASHR3), was shown to interact with AMS, suggesting the epigenetic regulation of AMS-ASHR3 during stamen development and function (Thorstensen et al., 2008). To gain further insight into the function of AMS, we performed a yeast two-hybrid screen to identify AMS-interacting proteins. The full-length cDNA of AMS was fused in-frame to the GAL4 DNA binding domain (AMS-BD) (Figure 5A) and used as the bait to screen an *Arabidopsis* stamen yeast two-hybrid library.

The bait construct showed no significant background interactions, and three candidate AMS interactors (At1g06170, At2g31210, and At3g15400) were identified. Yeast coexpressing AS2-BD and AS1-AD, which have previously been shown to interact (Xu et al., 2003; Phelps-Durr et al., 2005), was used as a positive control. Under stringent selection conditions (5 mM 3-amino-1,2,4-triazole), which require activation of two independent reporter genes, yeast cells containing the AMS-BD fusion construct together with the AD empty vector did not grow on selective media (Figure 5B). However, AtbHLH089 and AtbHLH091 proteins, as well as ATA20, were shown to interact with AMS in yeast cells (Figure 5). AtbHLH091 (*ES-RH2* [for *EMS1_SPL-reduced highly 2*] cluster) and AtbHLH089 (*ES-RH1* cluster) share 40% amino acid sequence identity and are found in a distinct clade in the bHLH phylogenetic tree (Heim et al., 2003; Li et al., 2006b). AtbHLH089 is expressed in the tapetum and microsporocytes (Wijeratne et al., 2007); *ATA20* is tapetal specific and encodes a protein with novel repeat sequences and a Gly-rich domain (Rubinelli et al., 1998). To verify the protein interactions observed in the yeast two-hybrid experiments, we assayed the interaction between these proteins in vitro using a pull-down system. N-terminal His-tag constructs for each putative interactor were expressed in *Escherichia coli* and incubated with AMS-GST–tagged bacterial fusion protein. The protein mixtures were affinity purified with glutathione-coupled particles, separated by SDS-PAGE, and analyzed for copurification of the His-labeled putative interacting proteins. It is evident from Figure 5C that AMS-GST interacts with AtbHLH089, AtbHLH091, and ATA20, respectively, but not with the HIS-tag (PET32a Vector) alone; this result therefore confirms that AMS

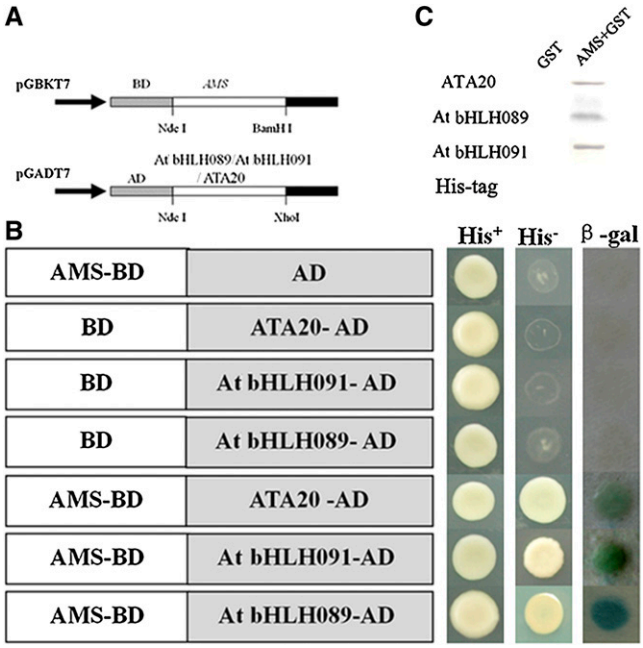

Figure 5. Proteins Interacting with AMS in Yeast and in Vitro.

(A) Schematic representations of the AMS-pGBKT7, ATA20-pGADT7, AtbHLH089-pGADT7, and AtbHLH091-pGADT7 fusion constructs.
(B) Interaction in yeast AH109 cells. ATA20, AtbHLH089, and AtbHLH091 were able to activate the expression of the His$^+$ and β-Gal reporter genes.
(C) Protein gel blot analysis of in vitro–translated full-length ATA20, AtbHLH089, and AtbHLH091 pulled down with bacterially expressed GST-AMS. GST alone was used as a negative control and showed no interaction with the His-tag.

protein can interact with AtbHLH089, AtbHLH091, and ATA20 (Figure 5C).

DISCUSSION

AMS Regulates Tapetal Secretion and PCD

AMS plays a critical role in the regulation of tapetal development and the formation of the pollen wall. In the *ams* mutant, the tapetum shows aberrant development and microspore degeneration occurs (see Supplemental Figures 3 and 4 online; Sorensen et al., 2003). We have shown that mutation of *AMS* results in a downregulation of gene expression commencing from meiosis and that many of these genes are associated with metabolic changes occurring in the tapetum and in the biosynthesis of pollen wall materials (Table 2; see Supplemental Tables 1 and 2 online). Many of these expression changes may be indirect effects of abnormal tapetal development; however, we have shown by qChIP-PCR that AMS selectively binds the promoters of 13 of these genes (Table 3), suggesting direct regulation of genes associated with tapetal metabolic processes. We have also demonstrated that AMS is able to bind in vitro to the hexa-nucleotide sequence known as the E-box

(CANNTG) (Figure 2; see Supplemental Figure 5 online), which is recognized by bHLH family proteins (Heim et al., 2003; Toledo-Ortiz et al., 2003).

Twenty-nine genes associated with lipid biosynthesis were downregulated in the *ams* mutant (see Supplemental Table 1 online), and *MS2*, which has been shown to be a fatty acyl reductase associated with sporopollenin biosynthesis (Aarts et al., 1997), shows significant downregulation in *ams*. Recently, the *ACOS5* gene was identified as functioning in a conserved biochemical pathway for the production of medium-chain fatty acyl-CoA for pollen wall development, and the *Arabidopsis acos5* mutant did not form obvious pollen exine (Souza et al., 2009).

The observed enlarged abnormal tapetum and aborted microspores without a normal pollen wall in the *ams* mutant is consistent with the regulatory role of AMS in lipid metabolism. From the tetrad stage, the tapetum starts depositing lipidic precursors onto the surface of microspore-derived cellulosic primexine, leading to the formation of sculptured exine. Subsequently, during the late stages of pollen development, the tapetum produces and secretes lipidic components of pollen coat/tryphine into exine cavities (Piffanelli et al., 1998; Blackmore et al., 2007). We have also observed that mutation of *TDR*, the putative ortholog of *AMS* in rice, causes abnormal lipid metabolism and pollen exine formation during anther development (Zhang et al., 2008). These data suggest a conserved role for AMS and TDR in regulating the metabolism of the lipidic molecules for pollen wall formation in both dicots and monocots.

Functional analysis of the ABC transporter WBC27, which is directly regulated by AMS, also supports a role for the AMS pathway in the transport of pollen wall materials. ABC transporters belong to the ABC superfamily, which uses the hydrolysis of ATP to transport a variety of substances across biological membranes. Knockout of *WBC27* results in a male sterile phenotype due to microspore degradation and a lack of functional pollen, and a recent independent TEM analysis of a *wbc27* mutant suggests that wall formation is abnormal (D. Ye, personal communication). WBC27 has also been shown to be associated with a number of proteins that exhibit changes in expression in the *ams* mutant (http://atted.jp/data/locus/At3g13220.shtml). There is predicted to be a direct connection between the MS2 protein and CYP703A2. Both of these are significantly downregulated in the *ams* mutant. This further strengthens the functional role of these components in the secretion and deposition of pollen wall materials.

We previously showed that the *MS1* gene is critical for pollen wall formation, late tapetal development, and tapetal PCD (Vizcay-Barrena and Wilson, 2006) and that a number of genes associated with metabolic changes, wall formation, and PCD show expression changes in the *ms1* mutant (Alves-Ferreira et al., 2007; Ito et al., 2007; Wijeratne et al., 2007; Yang et al., 2007). However, comparisons between the microarrays from *ams* and *ms1* mutants indicate that only ~42% of the genes are downregulated in both mutants (see Supplemental Figure 8, Supplemental Data Set 4, and Supplemental Table 4 online). These downregulated genes are predicted to act in lipid transport and metabolism, amino acid transport, secondary metabolite biosynthesis, and carbohydrate transport and metabolism. This suggests that although some components of late pollen development and expression changes show overlap in the downstream regulatory network, there are likely to be distinct roles for these two genes during anther development (Figure 6).

In addition to having a role in the formation of pollen wall materials, AMS also appears to affect the process of transport of wall materials from the tapetum into the locule for deposition onto the microspore and immature pollen grains. We have shown that AMS directly regulates the expression of two lipid transfer proteins, At3g51590 (LTP type 1) and At1g66850 (LTP type 2) (Figure 3). It is has been previously suggested that the anther-specific LTPs possibly participate in the transport of fatty acids and/or other sporopollenin precursors from the tapetum to the microspore during exine deposition (Xue et al., 1994). However, it has also been proposed that LTPs play a role in the initiation of PCD cascades by influencing mitochondrial transport (Crimi et al., 2006). Recent evidence indicates that saturated very-long-chain fatty acids ranging from C20:0 to C30:0 may be involved in activating ethylene biosynthesis (Qin et al., 2007) and that ethylene is a trigger in PCD (De Jong et al., 2002; Steffens and Sauter, 2005).

AMS may therefore act by regulating the induction and secretion of pollen wall components, alongside other genes associated with pollen wall formation, which are downregulated in *ams.* Alternatively, or additionally, AMS may act as a regulator of tapetal development and a facilitator of PCD by inducing expression of the LTP family of genes to alter mitochondrial permeability and induce tapetal PCD and thus indirectly affect pollen wall formation. A role for AMS in regulating PCD is akin to

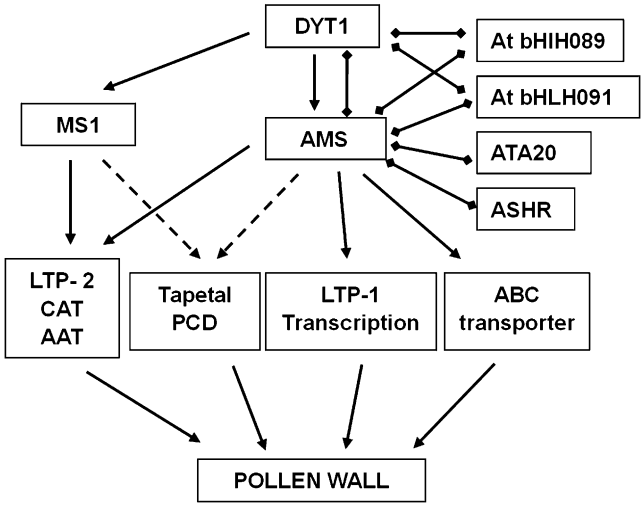

Figure 6. Model for the Role of AMS during Anther and Pollen Development.

AMS regulates a number of direct and downstream regulatory targets related to tapetal PCD and pollen wall formation and interacts with a number of proteins associated with anther and pollen development. This model provides an indication of the regulatory network for anther development. LTP, lipid transfer protein; CAT, carbohydrate transport and metabolism; AAT, amino acid transport and metabolism. Arrows indicate regulation; lines with diamond ends indicate interaction.

that proposed for the putative AMS ortholog in rice, *TDR*, which has been shown to directly regulate a Cys protease hypothesized to be associated with PCD (Li et al., 2006a; Zhang et al., 2006). Three Cys proteases are downregulated in the *ams* mutant (At4g16190, At1g06260, and At4g36880); however, it is not known whether these Cys proteases play a role in the induction of PCD.

AMS Forms a Protein Complex with Two bHLH Proteins and ATA20

Members of the bHLH gene family have frequently been shown to function as homodimers or heterodimers (Heim et al., 2003; Li et al., 2006b). Recently, the ASHR3 SET domain protein was shown to interact with the C-terminal region, which does not include the bHLH domain, of AMS (Thorstensen et al., 2008). *ASHR3* is expressed in the stamen and when overexpressed results in degeneration of anthers and male sterility, suggesting that ASHR3 may target AMS to chromatin and epigenetically regulate genes involved in stamen development (Thorstensen et al., 2008). To identify other components of the AMS protein complex, we screened a stamen-specific yeast two-hybrid library with the full-length AMS protein. This identified two bHLH (AtbHLH089 and AtbHLH091) proteins and the ATA20 protein, which interact with AMS; these interactions were subsequently confirmed by pull-downs assays. AtbHLH089 and AtbHLH091 have 40% amino acid identity and are in a distinct clade of the bHLH phylogenetic tree (Heim et al., 2003; Li et al., 2006b), alongside AtbHLH010/At2g31220. AtbHLH089/At1g06170 has been shown by in situ hybridization to be expressed in the tapetum and microspores during anther development (Wijeratne et al., 2007), and AtbHLH091 is expressed in the floral tissue, although vegetative expression is also seen (http://jsp.weigelworld.org/expviz/expviz.jsp?experiment=developmentandnormalization=absoluteandprobesetcsv=At2g31210andaction=Run). The AtbHLH010 gene is not present on the Affymetrix gene chip; however, RT-PCR analysis does not indicate that AtbHLH010 is florally expressed (Heim et al., 2003). The high level of sequence similarity and expression patterns suggests that AtbHLH089 and AtbHLH091 may be functionally redundant (Wijeratne et al., 2007). This is further supported by the ability of both bHLH proteins to interact with AMS; however, the expression profile suggests that AtbHLH010 is unlikely to act redundantly with them. It is interesting to note that DYT1 has also been shown to interact with these bHLH proteins by yeast two-hybrid assay (H. Ma, personal communication). AMS and DYT1 are both bHLH proteins with related structures. It is currently not known whether the AMS and DYT1 interactions with the bHLH proteins occur simultaneously and aid in the regulation of DYT1 and AMS activities or at different stages during tapetal development. However, it is interesting to speculate that they may function in a regulatory manner by competitively dimerizing at specific stages during development to regulate the tapetal transcriptome.

AMS was also shown to interact with the ATA20 protein. ATA20 has an N-terminal region with novel repeats, which are predicted to form a helical structure, and a C-terminal Gly-rich domain, which shows 53% similarity to a petunia Gly-rich cell wall protein and 48% identity to silk fibroin (Rubinelli et al., 1998). ATA20 shows strong stamen-specific expression; it has also been proposed that it may be secreted from the tapetal cells and transferred to the pollen during exine formation (Rubinelli et al., 1998).

AMS Regulatory Network

Expression analysis combined with qChIP-PCR has identified a number of direct and downstream regulatory targets of AMS, which has served to provide a fuller understanding of the regulatory role of AMS during pollen development (Figure 6). This has shown that AMS plays a fundamental role in the metabolic processes of pollen wall biosynthesis and that it may also be fundamental in maintaining normal tapetal development and the onset of tapetal PCD. In this manner, it appears to have an analogous function to *TDR*, its putative rice ortholog (Li et al., 2006a; Zhang et al., 2008). We have shown that AMS functions in a protein complex with two other bHLH proteins and an anther-specific protein (ATA20). AMS has also been shown to interact with the SET domain ASHR3 protein (Thorstensen et al., 2008). The future characterization of the role of chromatin modification of the AMS targets will provide valuable insight into the epigenetic regulation of pollen gene networks.

METHODS

Plant Material and Growth Conditions

Seeds of the SALK insertional mutant lines SALK_152147 and SALK_062317 (SIGnal; Alonso et al., 2003) and Columbia were obtained from the Nottingham Arabidopsis Stock Centre. Plant material was sown on Levington M3 supplemented with 0.2 gL^{-1} of Intercept and grown in controlled environmental chambers at 21 to 22°C under illumination of 167 $\mu mol \cdot m^{-2} \cdot s^{-1}$ with a 22-h photoperiod. The SALK_152147 and SALK_062317 lines were taken through a number of generations by crossing of male sterile lines to Columbia wild-type pollen and confirmed as carrying T-DNA insertions in the *AMS* and *WBC27* genes, respectively, by genotyping PCR (primer sequences are in Supplemental Table 5 online). Phenotypic analysis of the SALK_152147 mutant confirmed that the pollen development defects seen in the *ams* mutant (Steiner-Lange et al., 2003) were also observed in the *ams* SALK knockout. Alexander (1969) staining was used to test pollen viability.

Microarrays

Total RNA was isolated from three replicates of staged buds (PMII, bicellular, PMI, and PMC-meiosis) of the wild type and *ams* SALK_152147 mutant using the RNeasy kit (Qiagen). RNA quantity and quality were assessed with a Nanodrop ND-1000 spectrophotometer (Labtech) and an Agilent 2100 bioanalyzer (Agilent Technologies), respectively.

One microgram of total RNA was used to generate indirectly labeled probes with the Ambion Amino Allyl Message Amp II aRNA amplification kit (Amersham Biosciences) according to the manufacturer's protocol. Amino-allyl–labeled amplified RNA was labeled with cyanine 3-NHS-ester (Cy3) (Applied Biosystems) for *ams* and Alexafluor488-NHS-ester (AF488) (Molecular Probes) fluorescent dyes for wild-type Columbia samples.

Then, 0.5 μg of each Cy3- and Cy5-labeled aRNA was used for each channel of a two-color hybridization to in-house printed *Arabidopsis thaliana* oligonucleotide arrays (25K *Arabidopsis* oligosets; Ocimum

Biosolutions). Hybridizations were performed for 16 h at 50°C on a Tecan HS 4800 hybridization station (Tecan) with low agitation (period of 1.5 min agitation every 15 min for 16 h), using the Ocimum recommended solutions. Arrays were scanned with a GenePix 4200AL laser scanner (Axon-Molecular Devices).

Data Analysis and Gene Annotation

Primary image data for both dye channels was obtained for each array feature using GenePix Pro 6 software (Molecular Devices). Median intensities less the median local background intensity were used for each change as core data for further analysis. Features were filtered according to the following criteria: flag values <0, spots with diameter ≤60 and ≥110 μm, and median feature signal < background +2 SD of median background signal in both the Cy3 and the AF488 channels were excluded. The data were normalized using the Lowess algorithm (Yang et al., 2001). Data were expressed as a log2 (median intensity – background of CY3/median intensity –background of AF488) for each array feature.

Further gene expression analysis and gene ontology and metabolic pathway mapping were performed using J-Express Pro v2.7 software (Molmine) (Dysvik and Jonassen, 2001). SAM (Tusher et al., 2001) was performed to identify genes showing statistically significant fold changes in expression compared with the wild type and a false discovery rate of <5%.

qRT-PCR

Total RNA was isolated from staged buds (PMII, bicellular, PMI, and PMC-meiosis) using an RNeasy kit with DNaseI treatment (Qiagen). cDNA was synthesized using 5 μg of total RNA in a 20-μL reaction with oligo(dT) primers (Superscript III reverse transcriptase; Invitrogen). qRT-PCR analyses were performed using the Light Cycler 480 real-time PCR system (Roche Applied Science). Reactions contained the Brilliant SYBR Green QPCR Master Mix (Fermentas) in a final volume of 12 μL with 10 pM of the appropriate primers (see Supplemental Table 5 online) and 0.3 μL of cDNA. PCR cycling conditions for amplification were 95°C for 10 min followed by 40 cycles of 95°C for 30 s, 58°C for 1 min, and 72°C for 1 min. All samples were run at least in duplicate. Data acquisition and analyses were performed using the Roche Light Cycler software. Samples were normalized using *ACTIN7* expression and *PP2A3* (Czechowski et al., 2005); relative expression levels were determined compared with wild-type levels using the $2^{(-\Delta Ct)}$ analysis method.

TEM Analysis

Various stages of anthers from the wild type and the *ams* mutant were observed as previously described (Sorensen et al., 2003). Buds, at various stages of development (Ma, 2005), were fixed in 3% (w/v) paraformaldehyde and 0.25% glutaraldehyde in 0.2 N sodium phosphate buffer, pH 7.0, and were postfixed in 2% OsO_4 in PBS, pH 7.2. Following ethanol dehydration, samples were embedded in acrylic resin (London Resin Company). Ultrathin sections (50 to 70 nm) were double stained with 2% (w/v) uranyl acetate and 2.6% (w/v) lead citrate aqueous solution and examined with a JEM-1230 transmission electron microscope (JEOL) at 80 kV.

Preparation of AMS-Specific Polyclonal Antibodies and Specificity Analysis

After analyzing full-length *AMS* cDNA, a 522-bp *AMS*-specific fragment (415 to 936 bp) was amplified from *Arabidopsis* genomic DNA using the primer pairs AMS-SF (5′-aaaGGATCCGCTGAAGATCAGAACGTGGT-3′) and AMS-SR (5′-aaaAAGCTTTTGAGATCCTTTTCCTGACT-3′). The PCR product was cloned into the *Bam*HI and *Hin*dIII sites of the pET-32a vector (Novagen) to produce pET32a-AMS. The expression and purification of this fusion protein were performed according to the manufacturer's manual (Merck-Novagen), and the polyclonal antibodies against AMS were prepared as described by Huang et al. (2003).The specificity of the AMS antibody was tested by protein gel blot analysis for plant nuclei extracts of wild-type and *ams* mutant buds. Nuclei extracts were produced following the protocol that was used for the ChIP experiments except that the flower material was not fixed.

qChIP-PCR Analysis

The procedure for ChIP of AMS-DNA complexes in the wild-type *Arabidopsis* anther was modified from that of Bowler et al. (2004). Chromatin was isolated from 1.5 g of formaldehyde cross-linked buds (0.6 to 1.1 mm in length) expressing *AMS* (Sorensen et al., 2003). Immunoprecipitations with purified AMS-specific antiserum and preadsorption with protein A-Sepharose beads and without any serum were performed as described by Bowler et al. (2004). A small aliquot of untreated, sonicated chromatin was reversely cross-linked and used as the total input DNA control.

The oligonucleotides used for qPCR experiments are listed in Supplemental Table 5 online. Primers were synthesized by Shanghai Generay Biotech. Each primer pair was confirmed to yield a single band upon PCR amplification as assayed via agarose gel electrophoresis and dissociation curve analysis. Real-time PCR was performed on a Rotor-Gene RG3000A detection system (Corbett Research) using SYBR Green I master mix (Generay Biotech). All PCR experiments were conducted using 40 cycles of 94°C for 20 s, 42°C for 20 s, and 72°C for 20 s in a reaction mixture containing 10 pmole of each primer and 3 mM magnesium chloride and 0.5 μL DNA from ChIP or controls or 1 μL of input DNA diluted 100-fold (per biological replicate) as template. Each reaction was repeated three times. The mean Ct values of each gene were calculated and used for fold change calculations using the method described by Roter-Gene version 6.0 (Build 38) software. Quantification involved normalization of the Ct of each immune precipitation sample by subtracting the Ct of the NoAb control under the same conditions to obtain ΔCt values, $2^{(-\Delta Ct)}$, as the fold enrichment.

Random Binding Site Selection and Sequence Logos

The in vitro selection assay was based upon previous investigations for DNA protein binding sites (Blackwell and Weintraub, 1990; Thiesen and Bach, 1990; Sun and Baltimore, 1991; Ekker et al., 1992; Xue, 2005; Berger and Bulyk, 2006). As a source of protein, a C-terminal GST-AMS fusion protein was prepared from the full-length *AMS* ORF. Oligonucleotides containing 30-bp random sequences in the middle of a 70-bp template strand were prepared (Figure 3B) (Xue, 2005). The DNA binding/amplification was repeated four to five times, until abundant DNA was easily amplified (20 cycles) from the sample, but no detectable product was amplified from the control. The recovered DNA was then cloned and sequenced.

The sequence logos were created using the WebLOGOS (Web-based sequence logo generating application; Weblogo.berkeley.edu) program by providing the binding probabilities, for each base at each position in the sites. All logos were plotted in bits by converting logarithms to base 2.

Yeast Two-hybrid Assay

A yeast two-hybrid screen was conducted using the Gateway yeast two-hybrid system (Invitrogen). The full-length *AMS* coding region was cloned into pDEST32 and used to screen a stamen-specific library created in pEXP-AD502. Putatively positive clones were identified by sequencing.

The full-length *AMS* coding region was cloned into the pGBKT7 vector (Clontech) to create the fusion to the GAL4 DNA binding domain. The full-length ATA20, AtbHLH089, and AtbHLH091 coding regions were cloned into the pGADT7 vector (Clontech) to create the fusion to the GAL4 activation domain. Test constructs were transformed into the yeast strain AH109, and interactions were tested by His selection and X-Gal filter assay, following the manufacturer's instructions.

GST Pull Downs

Full-length ATA20, AtbHLH089, and AtbHLH091 were cloned into a pET28a (Novagen) and pET32a (His-tag control) vector and overexpressed in *Escherichia coli* as a fusion protein containing six N-terminal His residues. A C-terminal GST-AMS fusion protein was prepared from the full-length *AMS* ORF (pGEX-4T-1 vector). For each N-terminal His-tag construct, the putative interactor was incubated with AMS-GST tagged protein and then purified using GST and subjected to protein gel blot analysis using rabbit anti-6×His tag antibody (HuaAn Biotechnology Company) (Einarson and Orlinick, 2002).

EMSA

The recombinant GST-AMS protein was prepared as previously described using a pull-down process, and as a control, the GST protein translated from the pGEX-4T-1 control plasmid was added. The DNA fragments containing the E-box of the regulatory region of the ABC transporter *WBC27* were generated using PCR amplification with the following specific primers: 5′-TGTTCAAGTCAACAAATGCA-3′ and 5′-ATGAATGTAGGCTTGTGTT-3′. The DNA was labeled with digoxigenin using the DIG DNA labeling kit (LabKit) and purified on an 8% PAGE gel. The DNA binding reactions were performed according to Wang et al. (2002) and Li et al. (2006a) with minor modifications.

Accession Numbers

Sequence data from this article for the cDNA and genomic DNA of *AMS* can be found in the GenBank/EMBL data libraries under accession numbers NM_127244.4 and NC_003071, respectively. Accession numbers for the genes in this article are as follows: *ABC* transporter WBC27 (At1g66850); LTP type 2 (At3g13220); *LTP12* (At3g51590); AtbHLH089 (At1g06170); AtbHLH091(At2g31210); *MS2* (At3g11980); *ATA20* (At3g15400); *ATA7* (At4g28395); *ATA1* (At3g42960); *ATSTP2* (At1g07340); *PAB5* (At1g71770); *CYP704B1* (At1g69500); *CYP703A2* (At1g01280); and *ACOS5* (At1g62940).

Supplemental Data

The following materials are available in the online version of this article.

Supplemental Figure 1. qRT-PCR Analysis of Selected Genes Showing Changed Expression in *ams* Buds.

Supplemental Figure 2. GO Functional Grouping of All 549 Genes Showing >Log2 Fold Change in Expression and an FDR of <5% in the *ams* Mutant.

Supplemental Figure 3. Transverse Section Analysis of Anther and Microspore Development in the Wild Type (Col-0) and *ams* mutant.

Supplemental Figure 4. Transmission Electron Micrographs of Cross Sections of Wild-Type and *ams* Mutant Anthers at Stage 11.

Supplemental Figure 5. Random Binding Site Selection.

Supplemental Figure 6. Specificity Analysis of AMS Polyclonal Antibodies.

Supplemental Figure 7. Competitive Gel-Shift Assay of AMS with the Promoter Region of the ABC Transporter *WBC27.*

Supplemental Figure 8. A Venn Diagram Indicating the Overlap between Genes Identified as Being Downregulated in the *ams* and *ms1* Mutants.

Supplemental Table 1. Genes Putatively Involved in Lipid Metabolism, Carbohydrate and Amino Acid Transport, and Metabolism That Were Changed at <5% FDR by SAM Analysis and >Log2 Fold in *ams* Buds.

Supplemental Table 2. All Putative Transcription Factors Changed at <5% FDR by SAM Analysis and >Log2 Fold in *ams* Buds.

Supplemental Table 3. All Putative P450 Genes Changed at <5% FDR by SAM Analysis and >Log2 Fold in *ams* Buds.

Supplemental Table 4. Functional Classification of the 152 Genes Downregulated in Both *ams* and *ms1*.

Supplemental Table 5. Primers Used in This Study.

Supplemental Data Set 1. Genes with Altered Gene Expression in *ams* Buds Compared with the Wild Type as Identified by SAM Analysis (<5% FDR) and Showing a >Log2 Fold Change in Expression.

Supplemental Data Set 2. Predicted AMS Binding Motifs within 1-kb Promoter Region of Each Gene of 549 Changed Genes in *ams*.

Supplemental Data Set 3. Genes with Altered Gene Expression in *ams* Young Buds Compared with the Wild Type as Identified by SAM Analysis (<5% FDR) and Showing a >Log2 Fold Change That Were Also Changed in the *spl/nzz* and *ems1* Mutants (Wijeratne et al., 2007).

Supplemental Data Set 4. Genes with Altered Gene Expression in *ams* Buds Compared with the Wild Type (as Identified by SAM Analysis [<5% FDR] and Showing a >Log2 Fold Change in Expression) and Showing a Change in Expression in the *msl* Mutant (Alves-Ferreira et al., 2007; Yang et al., 2007).

ACKNOWLEDGMENTS

We acknowledge the Nottingham Arabidopsis Stock Centre for supply of seed stocks, Hong Ma for sharing unpublished results with us, Shu Wang, Shuling Li, and Yang Bian for help of the yeast two-hybrid analysis, and Mei Long for assistance with the semithin section analysis. Microarray hybridizations and bioinformatics support were kindly provided by Paddy Tighe (Post Genomic Technologies Facility, University of Nottingham). Work in Z.A.W.'s laboratory is supported by the Biotechnology and Biological Science Research Council. Work in D.-B.Z.'s laboratory is supported by funds from the National Basic Research Program of China (2009CB941500 and 2007CB108700), the National Natural Science Foundation of China (30725022, 30830014, and 90717109), the Science and Technology Commission of Shanghai Municipality, the Shanghai Leading Academic Discipline Project (B205), the China Postdoctoral Science Foundation (20090450706), the Shanghai Postdoctoral Scientific Program (09R21414300), and the International Cooperation project of Shanghai Science and Technology Committee (08540702700).

Received October 1, 2009; revised December 1, 2009; accepted December 25, 2009; published January 29, 2010.

REFERENCES

Aarts, M.G., Hodge, R., Kalantidis, K., Florack, D., Wilson, Z.A., Mulligan, B.J., Stiekema, W.J., Scott, R., and Pereira, A. (1997).

The Arabidopsis MALE STERILITY 2 protein shares similarity with reductases in elongation/condensation complexes. Plant J. **12:** 615–623.

Ageez, A., Kazama, Y., Sugiyama, R., and Kawano, S. (2005). Male-fertility genes expressed in male flower buds of *Silene latifolia* include homologs of anther-specific genes. Genes Genet. Syst. **80:** 403–413.

Alexander, M.P. (1969). Differential staining of aborted and nonaborted pollen. Stain Technol. **44:** 117–122.

Alonso, J.M., Stepanova, A.N., Leisse, T.J., Kim, C.J., Chen, H., Shinn, P., Stevenson, D.K., Zimmerman, J., Barajas, P., and Cheuk, R. (2003). Genome-wide insertional mutagenesis of *Arabidopsis thaliana.* Science **301:** 653–657.

Alves-Ferreira, M., Wellmer, F., Banhara, A., Kumar, V., Riechmann, J.L., and Meyerowitz, E.M. (2007). Global expression profiling applied to the analysis of Arabidopsis stamen development. Plant Physiol. **145:** 747–762.

Atchley, W.R., Terhalle, W., and Dress, A. (1999). Positional dependence, cliques, and predictive motifs in the bHLH protein domain. J. Mol. Evol. **48:** 501–516.

Belostotsky, D., and Meagher, R. (1993). Differential organ-specific expression of three poly(A)-binding-protein genes from *Arabidopsis thaliana.* Proc. Natl. Acad. Sci. USA **90:** 6686–6690.

Berger, M.F., and Bulyk, M.L. (2006). Protein binding microarrays (PBMs) for rapid, high-throughput characterization of the sequence specificities of DNA binding proteins. Methods Mol. Biol. **338:** 245–260.

Blackmore, S., Wortley, A.H., Skvarla, J.J., and Rowley, J.R. (2007). Pollen wall development in flowering plants. New Phytol. **174:** 483–498.

Blackwell, T.K., and Weintraub, H. (1990). Differences and similarities in DNA-binding preferences of MyoD and E2A protein complexes revealed by binding site selection. Science **250:** 1104–1110.

Bowler, C., Benvenuto, G., Laflamme, P., Molino, D., Probst, A.V., Tariq, M., and Paszkowski, J. (2004). Chromatin techniques for plant cells. Plant J. **39:** 776–789.

Canales, C., Bhatt, A.M., Scott, R., and Dickinson, H. (2002). EXS, a putative LRR receptor kinase, regulates male germline cell number and tapetal identityand promotes seed development in Arabidopsis. Curr. Biol. **12:** 1718–1727.

Crimi, M., Astegno, A., Zoccatelli, G., and Esposti, M.D. (2006). Pro-apoptotic effect of maize lipid transfer protein on mammalian mitochondria. Arch. Biochem. Biophys. **445:** 65–71.

Czechowski, T., Stitt, M., Altmann, T., Udvardi, M.K., and Scheible, W.R. (2005). Genome-wide identification and testing of superior reference genes for transcript normalization in Arabidopsis. Plant Physiol. **139:** 5–17.

De Jong, A.J., Yakimova, E.T., Kapchina, V.M., and Woltering, E.J. (2002). A critical role for ethylene in hydrogen peroxide release during programmed cell death in tomato suspension cells. Planta **214:** 537–545.

Dobritsa, A.A., Shrestha, J., Morant, M., Pinot, F., Matsuno, M., Swanson, R., Moller, B.L., and Preuss, D. (2009). CYP704B1 is a long-chain fatty acid {omega}-hydroxylase essential for sporopollenin synthesis in pollen of *Arabidopsis thaliana*. Plant Physiol. **151:** 574–589.

Dysvik, B., and Jonassen, I. (2001). J-Express: Exploring Gene Expression Data Using Java. (New York: Oxford University Press).

Einarson, M.B., and Orlinick, J.R. (2002). Identification of protein-protein interactions with glutathione S-transferase fusion proteins. In Protein-Protein Interactions: A Molecular Cloning Manual, J. Sambrook, P. MacCallum, and D. Russell, eds (Cold Spring Harbor, NY: Cold Spring Harbor Laboratory Press), pp. 37–57.

Ekker, S.C., Von Kessler, D.P., and Beachy, P.A. (1992). Differential DNA sequence recognition is a determinant of specificity in homeotic gene action. EMBO J. **11:** 4059–4072.

Garcia, O., Bouige, P., Forestier, C., and Dassa, E. (2004). Inventory and comparative analysis of rice and Arabidopsis ATP-binding cassette (ABC) systems. J. Mol. Biol. **343:** 249–265.

Glover, J., Grelon, M., Craig, S., Chaudhury, A., and Dennis, E. (1998). Cloningand characterization of *MS5* from Arabidopsis: A gene critical in male meiosis. Plant J. **15:** 345–356.

Goldberg, R.B., Beals, T.P., and Sanders, P.M. (1993). Anther development: Basic principles and practical applications. Plant Cell **5:** 1217–1229.

Goldberg, R.B., Sanders, P.M., and Beals, T.P. (1995). A novel cell-ablation strategy for studying plant development. Philos. Trans. R. Soc. Lond. B Biol. Sci. **350:** 5–17.

Heim, M.A., Jakoby, M., Werber, M., Martin, C., Weisshaar, B., and Bailey, P.C. (2003). The basic helix-loop-helix transcription factor family in plants: A genome-wide study of protein structure and functional diversity. Mol. Biol. Evol. **20:** 735–747.

Honys, D., and Twell, D. (2004). Transcriptome analysis of haploid male gametophyte development in Arabidopsis. Genome Biol. **5:** R85.

Hsieh, K., and Huang, A.H. (2007). Tapetosomes in *Brassica* tapetum accumulate endoplasmic reticulum-derived flavonoids and alkanes for delivery to the pollen surface. Plant Cell **19:** 582–596.

Huang, Y.H., Liang, W.Q., Pan, A.H., Zhou, Z.A., Huang, C., Chen, J. X., and Zhang, D.B. (2003). Production of FaeG, the major subunit of K88 fimbriae, in transgenic tobacco plants and its immunogenicity in mice. Infect. Immun. **71:** 5436–5439.

Ichihara, K., Kobayashi, N., and Saito, K. (2003). Lipid synthesis and acyl-CoA synthetase in developing rice seeds. Lipids **38:** 881–884.

Ito, T., Nagata, N., Yoshiba, Y., Ohme-Takagi, M., Ma, H., and Shinozaki, K. (2007). *Arabidopsis MALE STERILITY1* encodes a PHD-Type transcription factor and regulates pollen and tapetum development. Plant Cell **19:** 3549–3562.

Jasinski, M., Ducos, E., Martinoia, E., and Boutry, M. (2003). The ATP-binding cassette transporters: Structure, function, and gene family comparison between rice and Arabidopsis. Plant Physiol. **131:** 1169–1177.

Jiang, P.L., Wang, C.S., Hsu, C.M., Jauh, G.Y., and Tzen, J.T. (2007). Stable oil bodies sheltered by a unique oleosin in lily pollen. Plant Cell Physiol. **48:** 812–821.

Jung, K.H., Han, M.J., Lee, Y.S., Kim, Y.W., Hwang, I., Kim, M.J., Kim, Y.K., Nahm, B.H., and An, G. (2005). Rice Undeveloped Tapetum1 is a major regulator of early tapetum development. Plant Cell **17:** 2705–2722.

Kaul, M.L.H. (1988). Male sterility in higher plants. In Monograph on Theoretical and Applied Genetics, Vol. 10 (Berlin: Springer-Verlag).

Lemoine, R. (2000). Sucrose transporters in plants: Update on function and structure. Biochim. Biophys. Acta **1465:** 246–262.

Lebel-Hardenack, S., Ye, D., Koutnikova, H., Saedler, H., and Grant, S.R. (1997). Conserved expression of a TASSELSEED2 homolog in the tapetum of the dioecious *Silene latifolia* and *Arabidopsis thaliana.* Plant J. **12:** 515–526.

Li, N., et al. (2006a). The rice *Tapetum Degeneration Retardation* gene is required for tapetum degradation and anther development. Plant Cell **18:** 2999–3014.

Li, X., et al. (2006b). Genome-wide analysis of basic/helix-loop-helix transcription factor family in rice and Arabidopsis. Plant Physiol. **141:** 1167–1184.

Lu, B., Xu, C., Awai, K., Jones, A.D., and Benning, C. (2007). A small ATPase protein of Arabidopsis, TGD3, involved in chloroplast lipid import. J. Biol. Chem. **282:** 35945–35953.

Luo, B., Xue, X.Y., Hu, W.L., Wang, L.J., and Chen, X.Y. (2007). An ABC transporter gene of *Arabidopsis thaliana*, AtWBC11, is involved

in cuticle development and prevention of organ fusion. Plant Cell Physiol. **48:** 1790–1802.

Ma, H. (2005). Molecular genetic analyses of microsporogenesis and microgametogenesis in flowering plants. Annu. Rev. Plant Biol. **56:** 393–434.

Martinez-Garcia, J.F., Huq, E., and Quail, P.H. (2000). Direct targeting of light signals to a promoter element-bound transcription factor. Science **288:** 859–863.

Massari, M.E., and Murre, C. (2000). Helix-loop-helix proteins: Regulators of transcription in eucaryotic organisms. Mol. Cell. Biol. **20:** 429–440.

Mayfield, J.A., Fiebig, A., Johnstone, S.E., and Preuss, D. (2001). Gene families from the *Arabidopsis thaliana* pollen coat proteome. Science **292:** 2482–2485.

Mayfield, J.A., and Preuss, D. (2000). Rapid initiation of Arabidopsis pollination requires the oleosin-domain protein GRP17. Nat. Cell Biol. **2:** 128–130.

McCormick, S. (2004). Control of male gametophyte development. Plant Cell **16** (suppl.): S142–S153.

Morant, M., Jorgensen, K., Schaller, H., Pinot, F., Moller, B.L., Werck-Reichhart, D., and Bak, S. (2007). CYP703 is an ancient cytochrome P450 in land plants catalyzing in-chain hydroxylation of lauric acid to provide building blocks for sporopollenin synthesis in pollen. Plant Cell **19:** 1473–1487.

Millar, A.A., and Gubler, F. (2005). The *Arabidopsis GAMYB*-like genes, *MYB33* and *MYB65*, are microRNA-regulated genes that redundantly facilitate anther development. Plant Cell **17:** 705–721.

Nesi, N., Debeaujon, I., Jond, C., Pelletier, G., Caboche, M., and Lepiniec, L. (2000). The *TT8* gene encodes a basic helix-loop-helix domain protein required for expression of DFR and BAN genes in *Arabidopsis* siliques. Plant Cell **12:** 1863–1878.

O'Hara, P., Slabas, A.R., and Fawcett, T. (2001). Fatty acid synthesis in developing leaves of *Brassica napus* in relation to leaf growth and changes in activity of 3-oxoacyl-ACP reductase. FEBS Lett. **488:** 18–22.

Pacini, E., Franchi, G.G., and Hesse, M. (1985). The tapetum: Its form, function, and possible phylogeny in embryophyta. Plant Sys. Evol. **149:** 155–185.

Panikashvili, D., Savaldi-Goldstein, S., Mandel, T., Yifhar, T., Franke, R.B., Hofer, R., Schreiber, L., Chory, J., and Aharoni, A. (2007). The Arabidopsis DESPERADO/AtWBC11 transporter is required for cutin and wax secretion. Plant Physiol. **145:** 1345–1360.

Papini, A., Mosti, S., and Brighigna, L. (1999). Programmed-cell-death events during tapetum development of angiosperms. Protoplasma **207:** 213–221.

Phelps-Durr, T.L., Thomas, J., Vahab, P., and Timmermans, M.C.P. (2005). Maize rough sheath2 and its *Arabidopsis* orthologue ASYMMETRIC LEAVES1 interact with HIRA, a predicted histone chaperone, to maintain knox gene silencing and determinacy during organogenesis. Plant Cell **17:** 2886–2898.

Piffanelli, P., Ross, J.H.E., and Murphy, D.J. (1998). Biogenesis and function of the lipidic structures of pollen grains. Sex. Plant Reprod. **11:** 65–80.

Pollak, P.E., Vogt, T., Mo, Y., and Taylor, L.P. (1993). Chalcone synthase and flavonol accumulation in stigmas and anthers of *Petunia hybrida.* Plant Physiol. **102:** 925–932.

Qin, Y.M., Hu, C.Y., Pang, Y., Kastaniotis, A.J., Hiltunen, J.K., and Zhu, Y.X. (2007). Saturated very-long-chain fatty acids promote cotton fiber and *Arabidopsis* cell elongation by activating ethylene biosynthesis. Plant Cell **19:** 3692–3704.

Rea, P.A. (2007). Plant ATP-binding cassette transporters. Annu. Rev. Plant Biol. **58:** 347–375.

Robinson, K.A., Koepke, J.I., Kharodawala, M., and Lopes, J.M. (2000). A network of yeast basic helix-loop-helix interactions. Nucleic Acids Res. **28:** 4460–4466.

Rubinelli, P., Hu, Y., and Ma, H. (1998). Identification, sequence analysis and expression studies of novel anther-specific genes of *Arabidopsis thaliana.* Plant Mol. Biol. **37:** 607–619.

Sanchez-Fernandez, R., Davies, T.G., Coleman, J.O., and Rea, P.A. (2001). The *Arabidopsis thaliana* ABC protein superfamily, a complete inventory. J. Biol. Chem. **276:** 30231–30244.

Schiefthaler, U., Balasubramanian, S., Sieber, P., Chevalier, D., Wisman, E., and Schneitz, K. (1999). Molecular analysis of *NOZZLE*, a gene involved inpattern formation and early sporogenesis during sex organ development in*Arabidopsis thaliana.* Proc. Natl. Acad. Sci. USA **96:** 11664–11669.

Scott, R.J., Spielman, M., and Dickinson, H.G. (2004). Stamen structure and function. Plant Cell **16**(Suppl): S46–S60.

Shivanna, K.R., Cresti, M., and Ciampolini, F. (1997). Pollen development and pollen-pistil interaction. In Pollen Biotechnology for Crop Production and Improvement, K.R. Shivanna and V.K. Sawhney, eds (Cambridge, UK: Cambridge University Press), pp. 15–39.

Sorensen, A.M., Krober, S., Unte, U.S., Huijser, P., Dekker, K., and Saedler, H. (2003). The Arabidopsis *ABORTED MICROSPORES* (*AMS*) gene encodes a MYC class transcription factor. Plant J. **33:** 413–423.

Souza, C.D., Kim, S.S., Koch, S., Kienow, L., Schneider, K., McKim, S.M., Haughn, G.W., Kombrink, E., and Douglas, C.J. (2009). A novel fatty acyl-CoA synthetase is required for pollen development and sporopollenin biosynthesis in *Arabidopsis.* Plant Cell **21:** 507–525.

Steffens, B., and Sauter, M. (2005). Epidermal cell death in rice is regulated by ethylene, gibberellin, and abscisic acid. Plant Physiol. **139:** 713–721.

Steiner-Lange, S., Unte, U.S., Eckstein, L., Yang, C., Wilson, Z.A., Schmelzer, E., Dekker, K., and Saedler, H. (2003). Disruption of *Arabidopsis thaliana MYB26* results in male sterility due to non-dehiscent anthers. Plant J. **34:** 519–528.

Sun, X.H., and Baltimore, D. (1991). An inhibitory domain of E12 transcription factor prevents DNA binding in E12 homodimers but not in E12 heterodimers. Cell **64:** 459–470.

Thiesen, H., and Bach, C. (1990). Target Detection Assay (TDA): A versatile procedure to determine DNA blinding sites as demonstrated on SP1 protein. Nucleic Acids Res. **18:** 3203-9.

Thorstensen, T., Grini, P.E., Mercy, I.S., Alm, V., Erdal, S., Aasland, R., and Aalen, R.B. (2008). The Arabidopsis SET-domain protein ASHR3 is involved in stamen development and interacts with the bHLH transcription factor *ABORTED MICROSPORES* (*AMS*). Plant Mol. Biol. **66:** 47–59.

Toledo-Ortiz, G., Huq, E., and Quail, P.H. (2003). The Arabidopsis basic/helix-loop-helix transcription factor family. Plant Cell **15:** 1749–1770.

Truernit, E., Stadler, R., Baier, K., and Sauer, N. (1999). A male gametophyte–specific monosaccharide transporter in *Arabidopsis.* Plant J. **17:** 191–201.

Tusher, V.G., Tibshirani, R., and Chu, G. (2001). Significance analysis of microarrays applied to the ionizing radiation response. Proc. Natl. Acad. Sci. USA **98:** 5116–5121.

Vizcay-Barrena, G., and Wilson, Z.A. (2006). Altered tapetal PCD and pollen wall development in the Arabidopsis *ms1* mutant. J. Exp. Bot. **57:** 2709–2717.

Wang, H., Tang, W., Zhu, C., and Perry, S.E. (2002). A chromatin immunoprecipitation (ChIP) approach to isolate genes regulated by AGL15, a MADS domain protein that preferentially accumulates in embryos. Plant J. **32:** 831–843.

Wijeratne, A.J., Zhang, W., Sun, Y.J., Liu, W., Albert, R., Zheng, Z., Oppenheimer, D.G., Zhao, D.Z., and Ma, H. (2007). Differential gene

expression in Arabidopsis wild-type and mutant anthers: insights into anther cell differentiation and regulatory networks. Plant J. **52:** 14–29.

Wilson, Z.A., and Zhang, D.B. (2009). From Arabidopsis to rice: Pathways in pollen development. J. Exp. Bot. **60:** 1479–1492.

Wu, H.M., and Cheun, A.Y. (2000). Programmed cell death in plant reproduction. Plant Mol. Biol. **44:** 267–281.

Xu, L., Xu, Y., Dong, A.W., Sun, Y., Pi, L.M., and Huang, H. (2003). Novel *as1* and *as2* defects in leaf adaxial-abaxial polarity reveal the requirement for *ASYMMETRIC LEAVES1* and *2* and *ERECTA* functions in specifying leaf adaxial identity. Development **130:** 4097–4107.

Xue, G.P. (2005). A CELD-fusion method for rapid determination of the DNA-binding sequence specificity of novel plant DNA-binding proteins. Plant J. **41:** 638–649.

Xue, Y., Collin, S., Davies, D.R., and Thomas, C.M. (1994). Differential screening of mitochondrial cDNA libraries from male-fertile and cytoplasmic male-sterile sugar-beet reveals genome rearrangements at atp6 and atpA loci. Plant Mol. Biol. **25:** 91–103.

Yang, C.-Y., Vizcay-Barrena, G., Conner, K., and Wilson, Z.A. (2007). *MALE STERILITY1* is required for tapetal development and pollen wall biosynthesis. Plant Cell **19:** 3530–3548.

Yang, M.C., Ruan, Q.G., Yang, J.J., Eckenrode, S., Wu, S., McIndoe, R.A., and She, J.X. (2001). A statistical method for flagging weak spots improves normalization and ratio estimates in microarrays. Physiol. Genomics **7:** 45–53.

Yang, W.C., Ye, D., Xu, J., and Sundaresan, V. (1999). The *SPOROCYTELESS* gene of Arabidopsis is required for initiation of sporogenesis and encodes anovel nuclear protein. Genes Dev. **13:** 2108–2117.

Zhang, D.S., Liang, W.Q., Yuan, Z., Li, N., Shi, J., Wang, J., Liu, Y.M., Yu, W.J., and Zhang, D.B. (2008). *Tapetum Degeneration Retardation* is critical for aliphatic metabolism and gene regulation during rice pollen development. Mol. Plant **1:** 599–610.

Zhang, W., Sun, Y.L., Timofejeva, L., Chen, C., Grossniklaus, U., and Ma, H. (2006). Regulation of *Arabidopsis* tapetum development and function by *DYSFUNCTIONAL TAPETUM* (*DYT1*) encoding a putative bHLH transcription factor. Development **133:** 3085–3095.

Zhao, D.Z., Wang, G.F., Speal, B., and Ma, H. (2002). The *EXCESS-MICROSPOROCYTES1* gene encodes a putative leucine-rich repeat receptorprotein kinase that controls somatic and reproductive cell fates in the Arabidopsis anther. Genes Dev. **16:** 2021–2031.